Electronic Supplementary Information (ESI)

Field-induced slow relaxation of the magnetisation in an anionic heterotetranuclear[$Zn^{II}Re^{IV}_3$] system

Adrián Sanchis-Perucho, Carlos Rojas-Dotti, Nicolás Moliner and José Martínez-Lillo*

Instituto de Ciencia Molecular (ICMol)/Departament de Química Inorgànica, Universitat de València, c/ Catedrático José Beltrán 2, 46980, Paterna, Valencia, Spain.

Table of contents **page**

Synthesis of 1.

All chemicals were used as received. The precursor $(NBu_4)_2[ReCl_4(ox)]$ was prepared following the literature procedures indicated in the references No. 24 and 25 of the main text.

A solution of $(NBu_4)_2[ReCl_4(ox)]$ (202.5 mg, 0.225 mmol) in a isopropanol/MeCN (15 mL, 9:1, v/v) mixture was added to a solution of $Zn(ClO_4)_2 \cdot 6H_2O$ (27.9 mg, 0.075 mmol) in isopropanol (15 mL) under continuous stirring. The resulting pale green solution was allowed to evaporate at room temperature. Green needles of **1** were grown in one day, were filtered off and washed with cold isopropanol and diethyl ether. Yield: *ca*. 50%. Better crystals of **1** were obtained when a 1:1 Re/Zn molar ratio was used in the synthesis. Anal. Calcd. for $C_{70}H_{144}N_4O_{12}Cl_{12}Re_3Zn$ (**1**): C, 36.80; H, 6.40; N, 2.45. Found: C, 37.30; H, 7.00; N, 2.50. IR (KBr pellet/cm^{-1}): bands associated to the oxalate ligand are observed at 1712m, 1656vs and 812m.

Table S1. Summary of the crystal data for compound 1.

Compound	**1**
Formula	$C_{70}H_{144}N_4O_{12}Cl_{12}Re_3Zn$
M_r	2283.25
Crystal system	triclinic
Space group	$P\bar{1}$
a/Å	9.813(1)
b/Å	19.331(1)
c/Å	25.223(1)
α/°	84.45(1)
β/°	83.08(1)
γ/°	81.72(1)
V / Å^3	4684.8(5)
Z	2
D_c/g cm^{-3}	1.619
μ(Mo-K_α)/mm^{-1}	4.511
Goodness-of-fit on F^2	0.992
R_1 [$I > 2\sigma(I)$]	0.0195
wR_1 [$I > 2\sigma(I)$]	0.0478
$\Delta\rho_{max,\ min}$/e.Å^{-3}	2.388 and -0.902

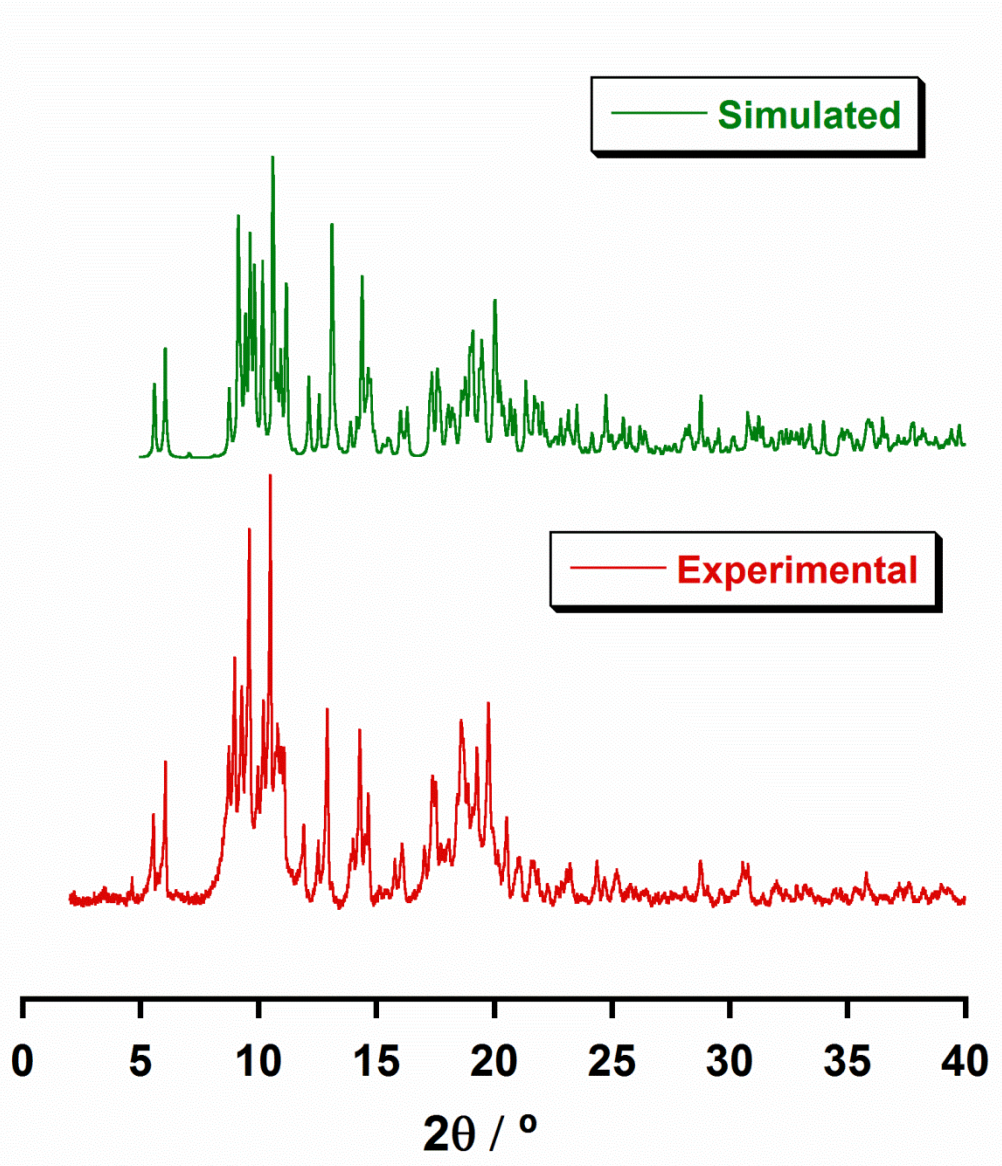

Figure S1. Plot of the simulated (green line) and experimental XRD (red line) patterns profile in the 2θ/° range 0–40° for **1**.

(a)

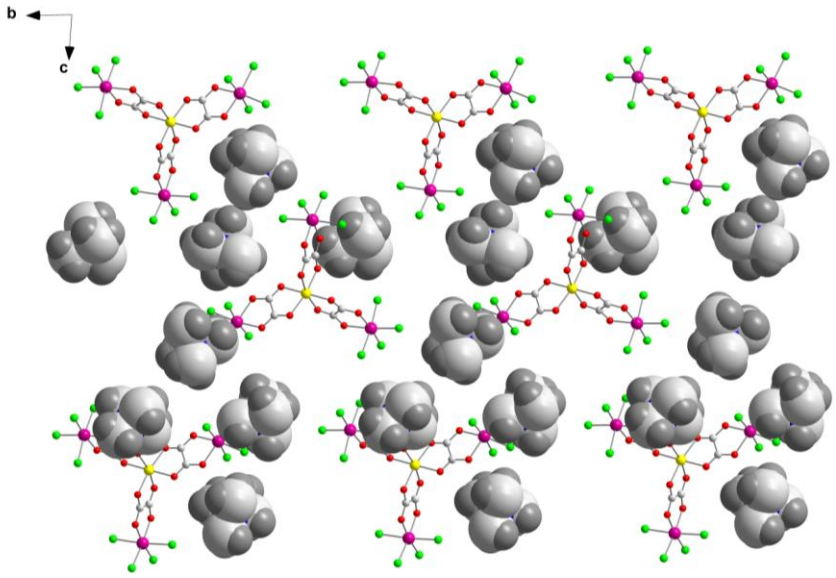

(b)

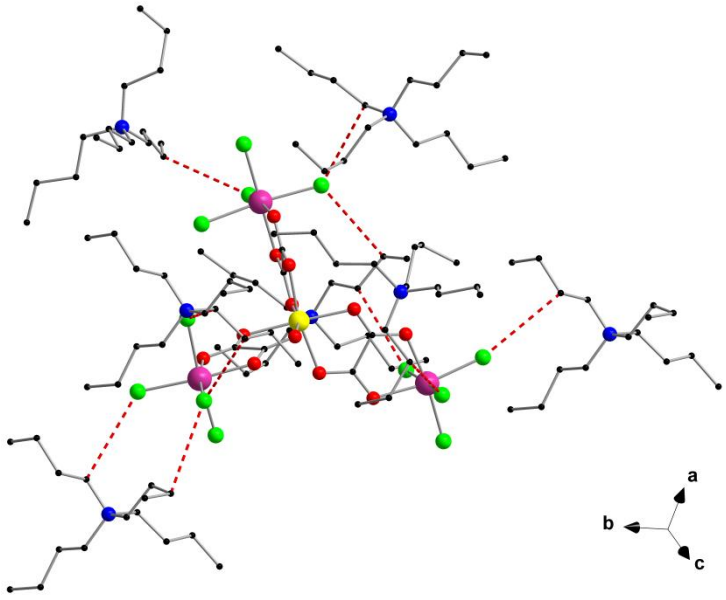

Figure S2. (a) View along the *a* crystallographic axis of the crystal packing of **1** showing the relative arrangement of the tetra-*n*-butylammonium cations (space-filling model) and the $[Zn\{ReCl_4(\mu\text{-}ox)\}_3]^{4-}$ anions. For the sake of clarity, only the $N(CH_2)_4$ skeleton of the tetra-*n*-butylammonium cations is shown. Colour code: pink, Re; yellow, Zn; green, Cl; red, O; blue, N; white, C; grey, H. (b) Detail of the weak C···Cl interactions between cations and anions in **1** (red dashed lines) with colour code: pink, Re; yellow, Zn; green, Cl; red, O; blue, N; black, C.

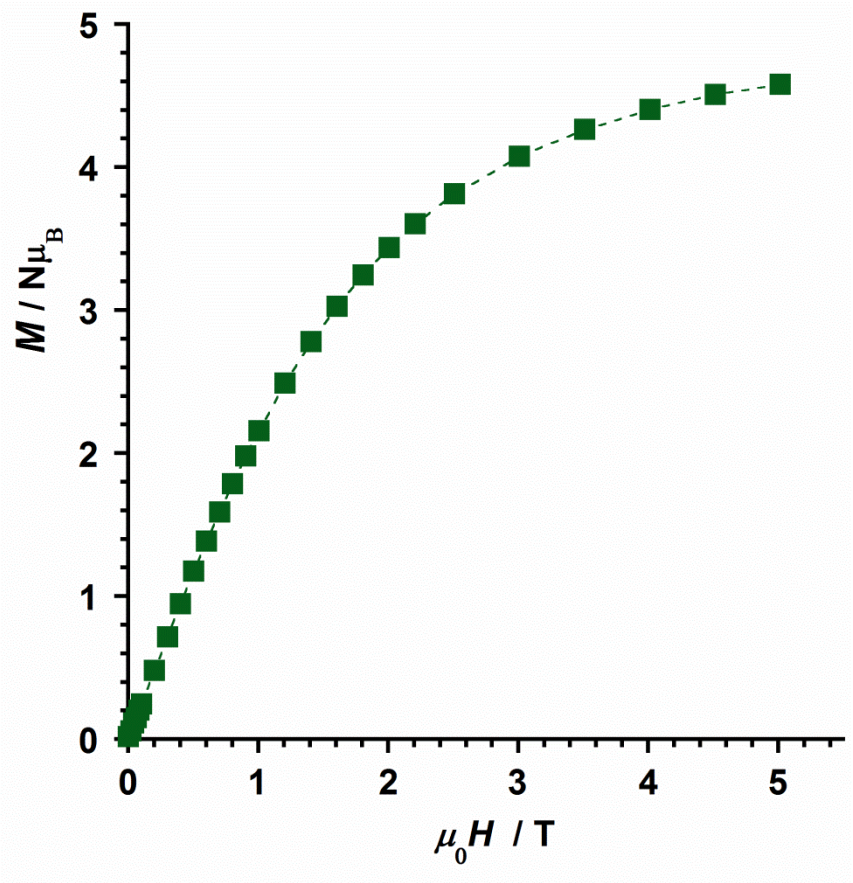

Figure S3. Plot of the variable-field magnetisation *versus* applied field at 2.0 K for **1**.

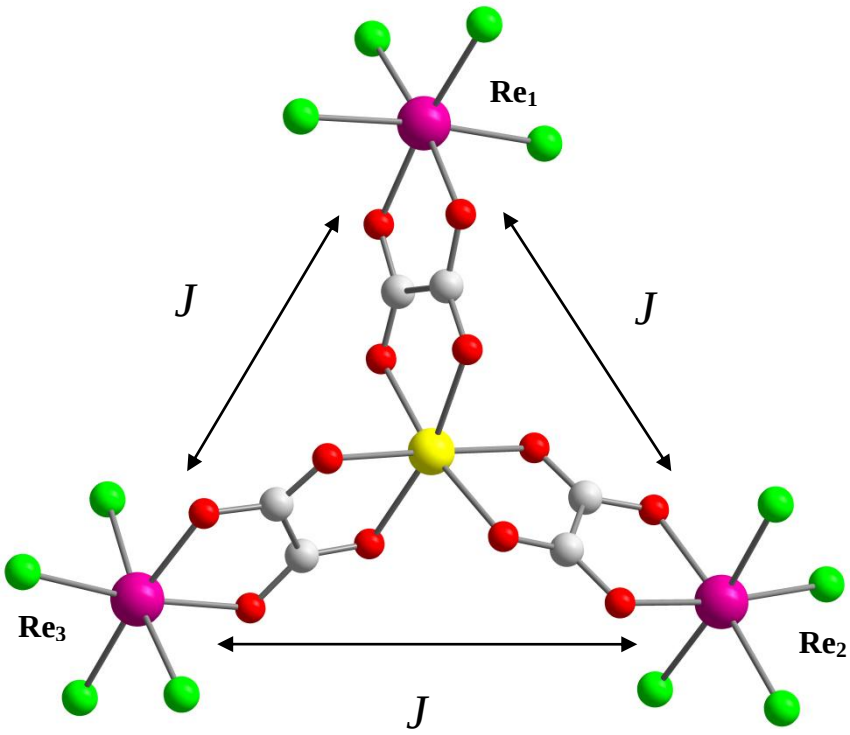

Figure S4. One *J* model employed to fit the experimental magnetic susceptibility data of compound **1**, where *J* is the exchange coupling constant for the intramolecular Re^{IV}–Re^{IV} interactions through the oxalate bridges. It is assumed that $g_{Re} = g_{Re1} = g_{Re2} = g_{Re3}$ and $D_{Re} = D_{Re1} = D_{Re2} = D_{Re3}$. Colour code: pink, Re; yellow, Zn; green, Cl; red, O; blue, N; white, C.

(a)

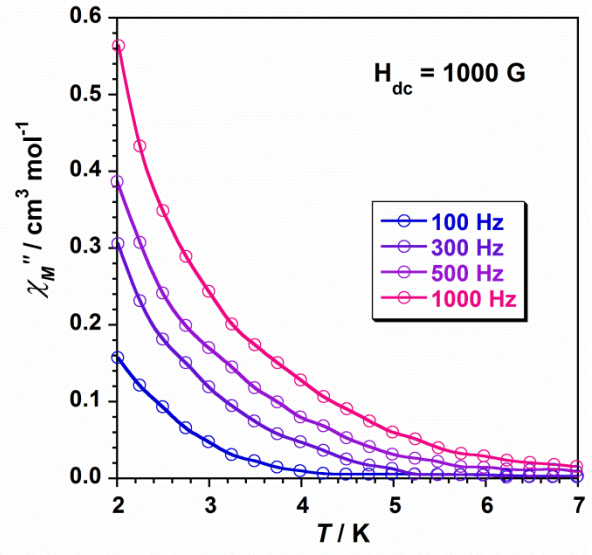

(b)

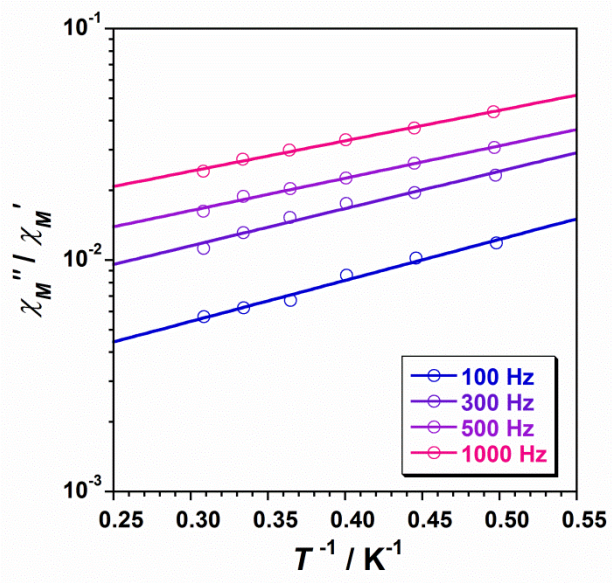

Figure S5. (a) Out-of-phase *ac* susceptibility *versus* temperature plot (χ''_M *vs*. *T*) for **1** at four different frequencies (100-1000 Hz range) under a dc field of 1000 G. (b) χ''_M/χ'_M *vs*. 1/*T* plot for **1**. The solid lines are the best-fit curves.

(a)

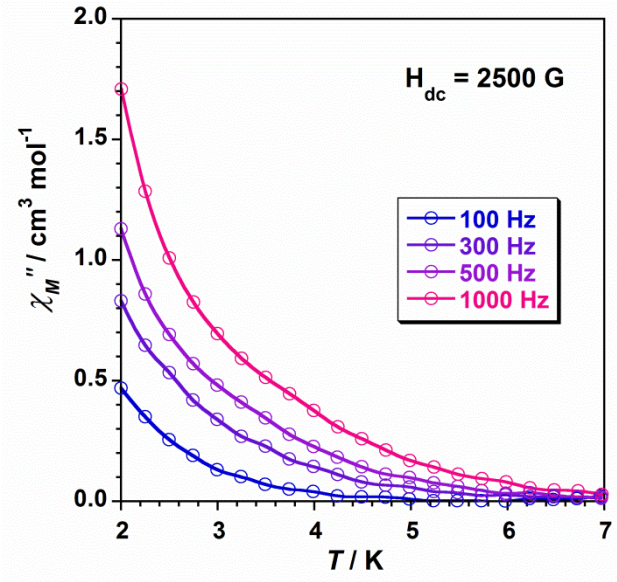

(b)

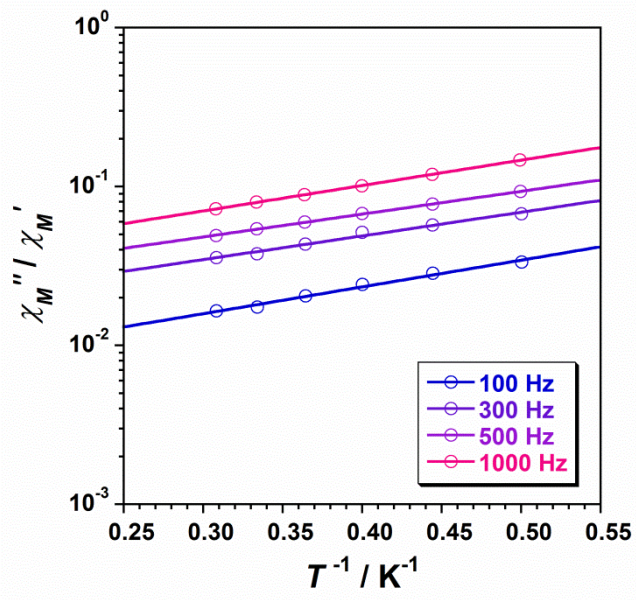

Figure S6. (a) Out-of-phase *ac* susceptibility *versus* temperature plot (χ''_M *vs*. *T*) for **1** at four different frequencies (100-1000 Hz range) under a dc field of 2500 G. (b) χ''_M/χ'_M *vs*. 1/*T* plot for **1**. The solid lines are the best-fit curves.

(a)

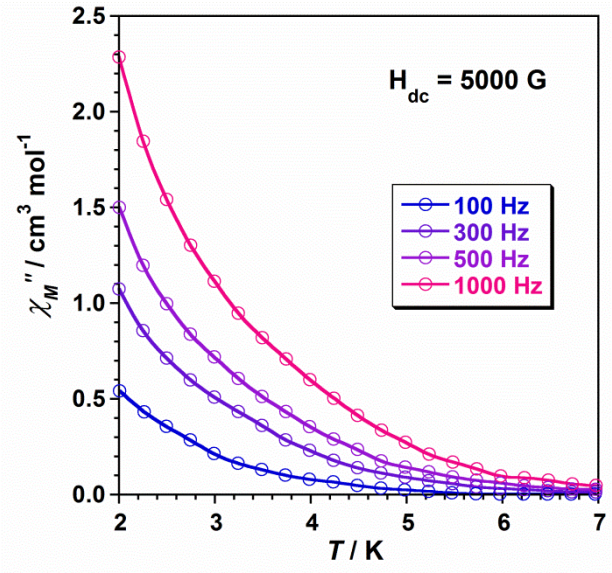

(b)

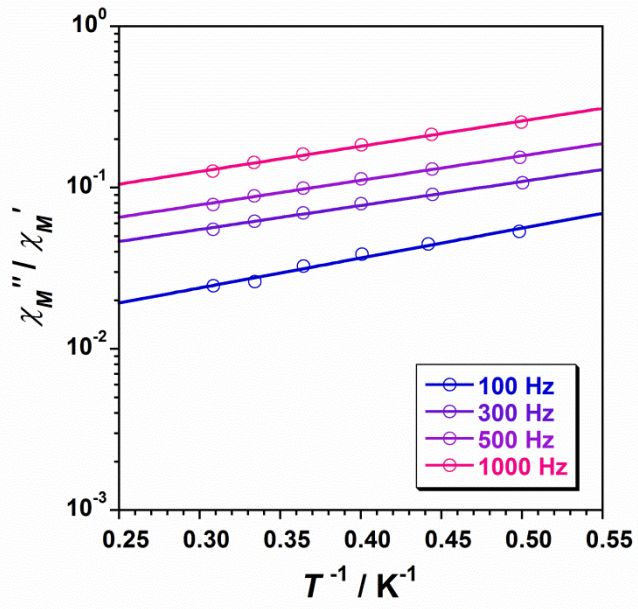

Figure S7. (a) Out-of-phase *ac* susceptibility *versus* temperature plot (χ''_M *vs*. *T*) for **1** at four different frequencies (100-1000 Hz range) under a dc field of 5000 G. (b) χ''_M/χ'_M *vs*. 1/*T* plot for **1**. The solid lines are the best-fit curves.

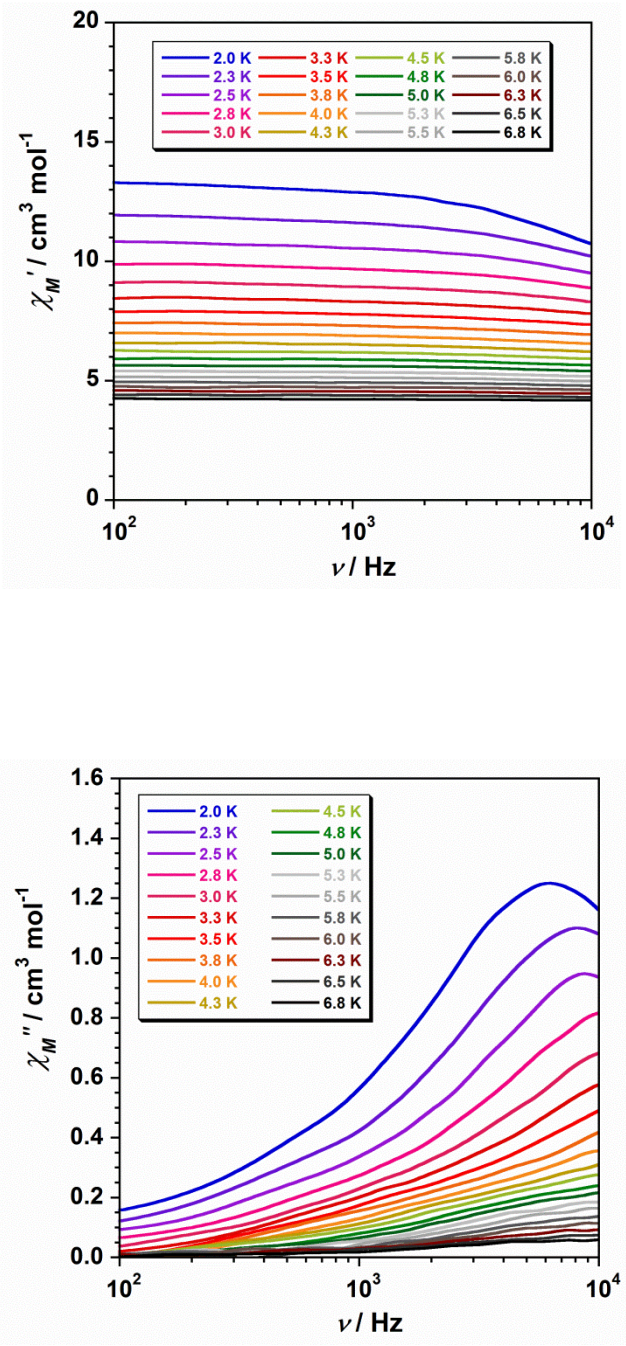

Figure S8. Frequency dependence of the in-phase (top) and out-of-phase (bottom) *ac* susceptibility signals for **1** under a dc field of 1000 G.

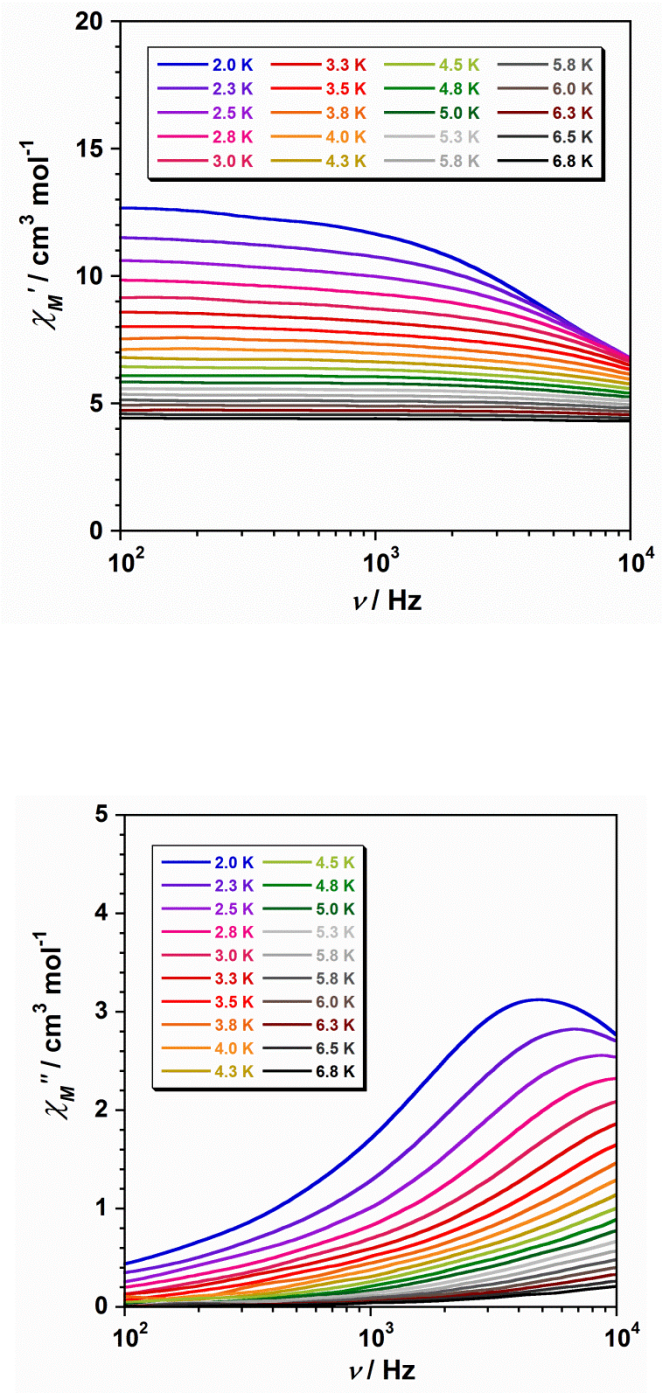

Figure S9. Frequency dependence of the in-phase (top) and out-of phase (bottom) *ac* susceptibility signals for **1** under a dc field of 2500 G.

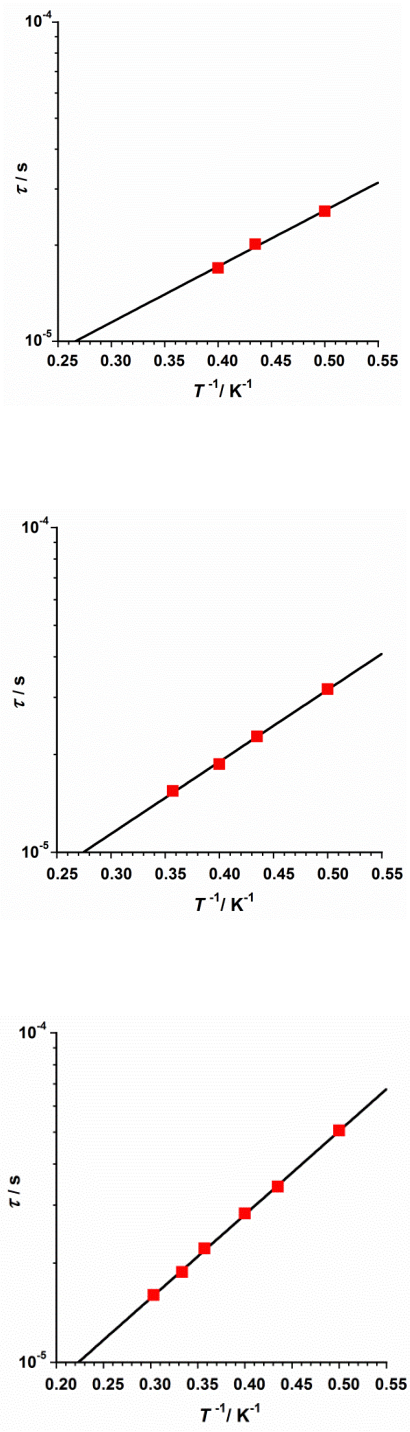

Figure S10. Arrhenius best-fit plots for **1** obtained by using the $\tau = \tau_o \exp(E^{\#}/k_B T)$ equation [where τ_o is the pre-exponential factor, τ is the relaxation time, $E^{\#}$ is the barrier to relaxation of the magnetisation and k_B is the Boltzmann constant] and the data from the *ac* measurements of the 1000 (top), 2500 (middle) and 5000 G (bottom) magnetic fields.

Table S2. Values of $E^{\#}$ and τ_0 obtained from different dc applied magnetic fields (H_{dc}) and equations (a and b) for **1**.

H_{dc} / G	$E^{\#}$ (K/cm^{-1}) [a]	τ_o (x 10^{-6}) [a] / s	$E^{\#}$ (K/cm^{-1}) [b]	τ_o (x 10^{-6}) [b] / s
1000	3.50 / 2.43	2.02	4.03 / 2.80	3.42
2500	3.70 / 2.57	5.66	5.00 / 3.48	2.68
5000	3.81 / 2.65	7.05	5.84 / 4.06	2.72

[a] Values obtained from the $\chi_M''/\chi_M' = 2\pi\nu\tau_o\exp(E^{\#}/k_BT)$ equation

[b] Values obtained from the $\tau = \tau_o\exp(E^{\#}/k_BT)$ equation